

$K\bar{K}$ -Continuum and Isoscalar Nucleon Form Factors

H.-W. Hammer^{a,1} and M.J. Ramsey-Musolf^{b,2}

^a TRIUMF, 4004 Wesbrook Mall, Vancouver, BC, Canada V6T 2A3

^b Department of Physics, University of Connecticut, Storrs, CT 06269, USA

Abstract

We analyse the isoscalar vector current form factors of the nucleon using dispersion relations. In addition to the usual vector meson poles, we account for the $K\bar{K}$ -continuum contribution by drawing upon a recent analytic continuation of KN scattering amplitudes. For the Pauli form factor all strength in the ϕ region is already given by the continuum contribution, whereas for the Dirac form factor additional strength in the ϕ region is required. The pertinent implications for the leading strangeness moments are demonstrated as well. We derive a reasonable range for the leading moments which is free of assumptions about the asymptotic behavior of the form factors. We also determine the ϕNN coupling constants from the form factor fits and directly from the $K\bar{K} \rightarrow N\bar{N}$ partial waves and compare the resulting values.

PACS: 14.20.Dh, 13.40.Gp, 11.55.Fv

Keywords: isoscalar nucleon form factors; dispersion relations; strangeness

¹email: hammer@triumf.ca

²email: mjrm@phys.uconn.edu

1 Introduction

The electromagnetic form factors of the nucleon are fundamental quantities that parametrize the structure of the nucleon as revealed by virtual photons. The understanding of these form factors is not only of importance in any theory or model of the strong interaction, but also serves as ingredient for precise tests of the Standard Model, e.g. in the Lamb shift measurements performed recently [1]. In the past, the form factors have been extracted from elastic electron-nucleon scattering experiments by means of the Rosenbluth separation. With the advent of the new continuous beam electron accelerators at Jefferson Lab, Bonn, Mainz, and NIKHEF, experiments with polarized beams and/or targets have become possible. These experiments allow for very precise measurements of those form factors which are suppressed in the Rosenbluth separation (see, e.g., Ref. [2] and references therein). In fact, a deviation from the well established dipole behavior has recently been observed at Jefferson Lab [3].

An essentially model independent tool to describe the form factors is given by dispersion theory [4, 5, 6]. Based on analyticity and causality, dispersion relations (DR) relate the real parts of the form factors to integrals involving their imaginary parts. The imaginary parts – or spectral functions – contain information on the contributions to the form factor dynamics made by various states in the hadronic spectrum. The quantum numbers of the current [$I^G(J^{PC})$] restricts the set of states which may contribute. For the isovector electromagnetic current [$1^+(1^{--})$], the lowest mass states are 2π , 4π , 6π , \dots , whereas for the isoscalar electromagnetic current [$0^-(1^{--})$] they are 3π , 5π , 7π , $2K$, \dots (cf. Refs. [7, 8]).

In principle, the electromagnetic spectral functions can be obtained from experimental data. In this respect, the low-mass spectral content of the isovector EM form factor has been well-understood for some time. Specifically, the contribution of the 2π -continuum, which is obtained from the electromagnetic form factor of the pion and the reaction $N\bar{N} \rightarrow \pi\pi$, has been determined by Höhler and Pietarinen [9]. This contribution manifests both a strong ρ -meson resonance as well as a pronounced un-correlated $\pi\pi$ continuum effect on the left wing of the resonance. The presence of the un-correlated continuum implies that the isovector EM form factors cannot be adequately represented by a simple vector meson dominance (VMD) picture [10]. Consequently, the 2π -continuum has been built into the spectral functions for the isovector nucleon form factors [11, 12] explicitly. The remaining strength in the isovector channel is then parametrized by three narrow excitations of the ρ meson.

The situation for the isoscalar form factors is less clear. As in the isovector case, one expects the low-mass states to generate both resonant and non-resonant continuum contributions. Historically, the first analyses of these form factors assumed that the isoscalar spectral functions can be parametrized solely by sharp vector meson resonances. Although such an approach does not produce the correct singularity structure for the form

factors [13], an adequate fit to EM data can nevertheless be obtained [11, 12]. Such fits require at least two closely-lying resonances (*e.g.*, ω and ϕ) with opposite sign residues in order to generate the observed dipole behavior of the form factors. A third resonance (denoted by S' in Ref. [11]) is included in order to obtain an acceptable χ^2 . The S' effectively summarizes higher-mass spectral strength. One surprising implication of the VMD analysis is a large value for the ϕ -nucleon coupling $g_{\phi NN}/g_{\omega NN} \approx -1/2$. This evidence for significant OZI-violation [14] suggests large moments for the strange vector form factors as well [15].

Subsequent studies have examined the validity of the VMD *ansatz* for the isoscalar form factors. The authors of Ref. [16] computed the un-correlated 3π continuum to leading order in chiral counting. They find no evidence for continuum enhancement as occurs for the 2π contribution to the isovector form factors.³ The authors of Ref. [17] argued that the VMD analyses neglect important contributions from a correlated $\rho\pi$ resonance which sits on top of the 3π continuum. It is argued in Ref. [17] that the effect of the $\rho\pi$ exchange can be parametrized by a single pole at $t = (1.12 \text{ GeV})^2$ with a residue fixed from the Bonn potential. A fit to isoscalar form factor data, with this effective $\rho\pi$ singularity included, leads to a significantly smaller ϕ -nucleon coupling than obtained in Refs. [11, 12]. To the extent that the $\rho\pi$ resonance does not couple to $\bar{s}\gamma_\mu s$, one infers considerably smaller values for the strangeness moments than obtained in Ref. [15]. It was noted in Ref. [18], however, that $\langle \rho\pi | \bar{s}\gamma_\mu s | 0 \rangle$ does not vanish, since the ϕ decays to $\rho\pi$ 12% of the time. Thus, the inclusion of the $3\pi \leftrightarrow \rho\pi$ resonance need not imply small strangeness moments.

In the wake of these analyses, several questions pertaining to the isoscalar EM and strangeness vector current spectral content remain:

- (i) Does any evidence exist among EM or strong interaction data for large OZI violation in the nucleon?
- (ii) Does the VMD picture give an accurate representation of the isoscalar EM spectral functions?
- (iii) To what extent does our knowledge of the isoscalar EM spectral functions constrain predictions for the strange quark vector current form factors and their leading moments?

In this paper, we address these issues by concentrating on the role of the $K\bar{K}$ -continuum. In analogy to analyses of the 2π -continuum for the isovector form factors, we introduce the $K\bar{K}$ -continuum into the analysis of the isoscalar ones and study the nature of the ϕ strength in detail. No additional parameters are introduced because this contribution is obtained from an analytic continuation of experimental KN scattering amplitudes and $e^+e^- \rightarrow K\bar{K}$ data [8]. In particular:

³The multi-pion contributions could, however, be enhanced by resonance effects [18].

- (a) We compare the ϕNN couplings derived from the $K\bar{K} \rightarrow N\bar{N}$ partial waves with those obtained from the original VMD analyses of the electromagnetic nucleon form factors and comment on the validity of the OZI rule. We find that strong interaction data imply large values for the $g_{\phi NN}$, in disagreement with the conclusions of Ref. [17].
- (b) We re-fit the isoscalar EM form factors under various scenarios used in Refs. [11, 12, 17] but also including the continuum $K\bar{K}$ contribution explicitly. Our fits determine the phase of the latter, which cannot be obtained from strong interaction and e^+e^- data alone, as well as the stable resonance contributions to the form factors. We find that the $K\bar{K}$ contribution, which contains a ϕ -resonance, accounts for nearly all the ϕ -strength in the isoscalar Pauli form factor, but that additional ϕ -strength is required in the isoscalar Dirac form factor.
- (c) Based on the analysis of (b), we argue that the the VMD approach represents an effective parameterization, but leads to erroneous values for the ϕ nucleon couplings.
- (c) We demonstrate the pertinent implications for the nucleon's strange vector form factors.

Our discussion of these points is organized as follows. In the next section, we briefly review the necessary formalism and dispersion relations. In Section 3, we derive ϕNN coupling constants from the $K\bar{K} \rightarrow N\bar{N}$ partial waves of Ref. [8]. The spectral content of the isoscalar form factors is analysed in Section 4. Finally, we demonstrate the consequences of our analysis for pole models of nucleon strangeness in Section 5 and conclude in Section 6.

2 Dispersion Relations

The vector current form factors of the nucleon, $F_1(t)$ and $F_2(t)$, are defined by:

$$\langle N(p') | j_\mu | N(p) \rangle = \bar{u}(p') \left[F_1(t) \gamma_\mu + \frac{iF_2(t)}{2m_N} \sigma_{\mu\nu} (p' - p)^\nu \right] u(p). \quad (1)$$

where $u(p)$ is the spinor associated with the nucleon state $|N(p)\rangle$ and $t = q^2 = (p' - p)^2$ is the four-momentum transfer. We consider two cases for j_μ : (i) the strange vector current $\bar{s}\gamma_\mu s$ and (ii) the isoscalar electromagnetic current $j_\mu^{(I=0)}$. Since the nucleon carries no net strangeness, F_1^s must vanish at zero momentum transfer, whereas $F_1^{(I=0)}$ is normalized to the isoscalar electromagnetic charge of the nucleon, $F_1^{(I=0)}(0) = 1/2$. Both currents couple

to the same intermediate states because they have the same quantum numbers [7, 8]. We use a subtracted dispersion relation (DR) for F_1 and an unsubtracted one for F_2 ,

$$F_1(t) = F_1(0) + \frac{t}{\pi} \int_{9m_\pi^2}^{\infty} \frac{\text{Im } F_1(t')}{t'(t' - t)} dt', \quad (2)$$

$$F_2(t) = \frac{1}{\pi} \int_{9m_\pi^2}^{\infty} \frac{\text{Im } F_2(t')}{t' - t} dt'. \quad (3)$$

The lower limit of integration is given by the threshold of the lightest intermediate state contributing to the form factors, the 3π state. In the VMD analyses of the isoscalar electromagnetic form factors (see, e.g., Refs. [11, 12]), their imaginary parts are parametrized by narrow vector meson resonances as,⁴

$$\text{Im } F_i(t) = \pi \sum_{j=\omega, \phi, S'} a_j^i \delta(t - m_j^2). \quad (4)$$

For a successful description of the data the ω , the ϕ , and a fictitious third S' resonance at $m_{S'} = 1.6$ GeV are needed. Although the S' can be identified with the $\omega(1600)$ or the $\phi(1680)$ [19], it effectively accounts for the strength in the high mass region. With the DR's, Eqs. (2, 3), this leads to the usual pole parametrizations,

$$F_1(t) = F_1(0) + \sum_{j=\omega, \phi, S'} \frac{t}{m_j^2} \frac{a_j^1}{m_j^2 - t}, \quad (5)$$

$$F_2(t) = \sum_{j=\omega, \phi, S'} \frac{a_j^2}{m_j^2 - t}. \quad (6)$$

The residues a_j^i are then fitted to the form factor data. In contrast to the isovector nucleon form factors, no continuum contributions are necessary to obtain successful fits. Based on these fits, the phenomenology of $\phi - \omega$ -mixing, and the known flavor content of the ω and ϕ , predictions for the strange vector form factors have been made [15, 20, 21]. However, the coupling of the S' to the strange vector current is uncertain. Because the flavor content of the S' is unknown, its coupling to $\bar{s}\gamma_\mu s$ has been inferred in Refs. [15, 20] from *ad hoc* assumptions about the asymptotic behavior of the strangeness form factors. Unfortunately, the leading moments of the strange form factors are very sensitive to the assumed asymptotic behavior [21, 22]. We present a possible solution to this problem in Section 5. First, we focus on the $K\bar{K}$ -continuum contribution for isoscalar nucleon form factors.

⁴Note that in Refs. [11, 12] an unsubtracted dispersion relation has been used for F_1 as well.

3 $K\bar{K}$ -Continuum

The $K\bar{K}$ contribution to the imaginary part of the isoscalar form factors is given by [7, 8]

$$\text{Im } F_1^{(a)}(t) = \text{Re} \left\{ \left(\frac{m_N q_t}{4p_t^2} \right) \left[\frac{E}{\sqrt{2}m_N} b_1^{1/2, -1/2}(t) - b_1^{1/2, 1/2}(t) \right] F_K^a(t)^* \right\}, \quad (7)$$

$$\text{Im } F_2^{(a)}(t) = \text{Re} \left\{ \left(\frac{m_N q_t}{4p_t^2} \right) \left[b_1^{1/2, 1/2}(t) - \frac{m_N}{\sqrt{2}E} b_1^{1/2, -1/2}(t) \right] F_K^a(t)^* \right\}, \quad (8)$$

with

$$p_t = \sqrt{t/4 - m_N^2}, \quad q_t = \sqrt{t/4 - m_K^2}, \quad \text{and} \quad E = \sqrt{t}/2. \quad (9)$$

The superscript a denotes s or $(I = 0)$ for strange and isoscalar electromagnetic form factors, respectively. $F_K^a(t)$ represents the kaon form factor in the respective channel,

$$\langle 0 | j_\mu^{(a)} | K(k) \bar{K}(\bar{k}) \rangle = (k - \bar{k})_\mu F_K^a(t), \quad (10)$$

whereas the $b_1^{1/2, \pm 1/2}$ are the $J = 1$ partial waves for $K\bar{K} \rightarrow N\bar{N}$ [7, 8]. Once these imaginary parts are determined, the contribution of the $K\bar{K}$ -continuum to the form factors is obtained from the DR's, Eqs. (2, 3). For $t \geq 4m_N^2$ the partial waves are bounded by unitarity,

$$|b_1^{1/2, \pm 1/2}(t)| \leq 1. \quad (11)$$

Eq. (11), however, does not hold in the unphysical region, $4m_K^2 \leq t \leq 4m_N^2$. Recently, the $b_1^{1/2, \pm 1/2}$ in the unphysical region have been determined from an analytic continuation of KN -scattering amplitudes [8]. The resulting partial waves are shown in Fig. 1. The striking feature is a clear resonance structure at threshold in $b_1^{1/2, 1/2}$, which presumably is the ϕ resonance. However, this resonance is not seen in $b_1^{1/2, -1/2}$ although it is not forbidden by the quantum numbers of the ϕ . In a simple resonance model this behavior is recovered when the vector ($g_{\phi NN}^1$) and tensor ($g_{\phi NN}^2$) couplings of the ϕ meson to the nucleon are equal and have opposite signs. This can be seen from the following parametrizations [23, 8],

$$\begin{aligned} b_1^{1/2, 1/2}(t) &= \frac{2q_t^2}{\sqrt{t}} \frac{2R_+^\phi}{m_\phi^2 - t - im_\phi \Gamma_\phi h_\phi(t)}, \\ b_1^{1/2, -1/2}(t) &= q_t^2 \frac{2R_-^\phi}{m_\phi^2 - t - im_\phi \Gamma_\phi h_\phi(t)}, \end{aligned} \quad (12)$$

with

$$\begin{aligned} R_+^\phi &= -\frac{2m_N}{3} \frac{g_{\phi K\bar{K}}}{4\pi} \left(g_{\phi NN}^1 + \frac{m_\phi^2}{4m_N^2} g_{\phi NN}^2 \right), \\ R_-^\phi &= -\frac{2\sqrt{2}}{3} \frac{g_{\phi K\bar{K}}}{4\pi} \left(g_{\phi NN}^1 + g_{\phi NN}^2 \right), \end{aligned} \quad (13)$$

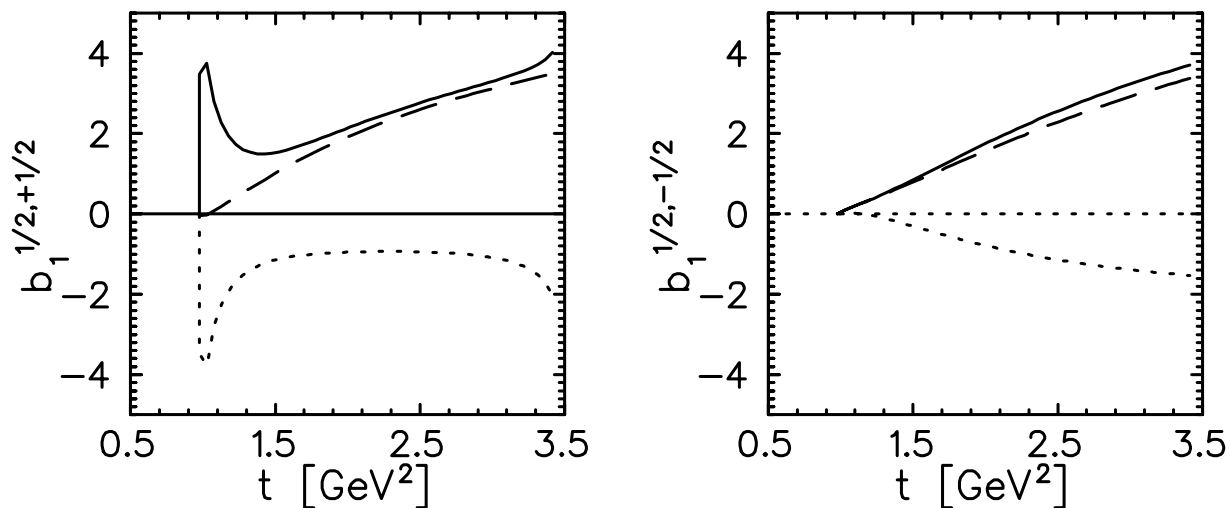


Figure 1: $b_1^{1/2, \pm 1/2}$ in the unphysical region, $4m_K^2 \leq t \leq 4m_N^2$, obtained from an analytic continuation of KN scattering amplitudes [8].

where Γ_ϕ is the total width of the ϕ and $h_\phi(t) = t/m_\phi^2$ [24]. The $\phi K \bar{K}$ coupling is obtained from the partial width of the $\phi \rightarrow K \bar{K}$ decay [23],

$$|g_{\phi K \bar{K}}| = 4.10 \pm 0.28. \quad (14)$$

We have fitted the expressions from Eqs. (12, 13) to the absolute values of the amplitudes from the analytic continuation (see Fig. 1) in order to determine the vector and tensor ϕNN couplings $g_{\phi NN}^1$ and $g_{\phi NN}^2$, respectively. Since the $b_1^{1/2, \pm 1/2}$ from the analytic continuation contain substantial nonresonant contributions, we only fit the region from the $K \bar{K}$ threshold to about 1.5 GeV where the ϕ resonance is dominating. Furthermore, we force $g_{\phi NN}^2 = -g_{\phi NN}^1$ to improve the stability of the fit. The resulting coupling constants are given in Table 1. We used two scenarios for our fits: (a) the width of the ϕ is taken from the particle data group [19] and (b) the width is fitted together with the coupling constant. The results for both scenarios agree within the error bars. Furthermore, $g_{\phi NN}^1$ agrees with the value obtained from the dispersion analysis of the electromagnetic nucleon form factors [12], while the values for $g_{\phi NN}^2$ are in variation. The discrepancy in $g_{\phi NN}^2$ is due to our constraint $g_{\phi NN}^2 = -g_{\phi NN}^1$. When we omit this constraint, $g_{\phi NN}^2 \approx 4.0$ is similar to the value of Ref. [12], however, the quality of the fit at threshold is not satisfactory. The size of the ϕNN coupling constants in both scenarios is of the same order as in pole analyses and therefore implies a large OZI-violation as well.

We believe that extracting the coupling constants from the partial waves rather than electromagnetic pole analyses is the more sensible procedure for at least three reasons.

Scenario	$g_{\phi NN}^1$	$g_{\phi NN}^2$
(a)	-7.4 ± 1.46	7.4 ± 1.46
(b)	-9.6 ± 2.44	9.6 ± 2.44
Ref. [12]	-9.16 ± 0.23	2.01 ± 0.33

Table 1: ϕNN coupling constants $g_{\phi NN}^2 = -g_{\phi NN}^1$ as obtained from a fit of Eqs. (12, 13) to the partial waves from Fig. 1. First two rows give our results for scenarios (a): $\Gamma = 4.43$ MeV [19] and (b) $\Gamma = 16 \pm 10$ MeV from fit. Last row gives the result of Ref. [12].

First, in the VMD form factor analyses, one effectively summarizes the sum over a variety of intermediate state contributions by a few sharp resonances. The residues in this case may include the effects of both true resonances as well as non-resonant continuum contributions.

Second, the EM form factor data exist only in the space-like domain and, thus, do not manifest any resonance structure explicitly. The KN partial waves, on the other hand, have been analytically continued into the time-like region where an isolated resonance structure is apparent (see Fig. 1).

Finally, the resonating contribution from a given intermediate state may not be adequately represented by a simple VMD *ansatz*. To see why, consider the $K\bar{K}$ contributions to the isoscalar EM form factors, $F_i^{K\bar{K}}$. We have also fitted these contributions (cf. Eqs. (7, 8)) with an effective ϕ pole,

$$\begin{aligned}
F_1^{K\bar{K}}(t) &= \frac{t}{m_\phi^2} \frac{\tilde{g}_{\phi NN}^1}{m_\phi^2 - t} \frac{m_\phi^2}{f_\phi}, \\
F_2^{K\bar{K}}(t) &= \frac{\tilde{g}_{\phi NN}^2}{m_\phi^2 - t} \frac{m_\phi^2}{f_\phi},
\end{aligned} \tag{15}$$

where $f_\phi = 13$ is obtained from the width of the leptonic decay $\phi \rightarrow e^+e^-$. We find the following effective coupling constants:

$$\tilde{g}_{\phi NN}^1 = 1.32 \pm 0.01 \quad \text{and} \quad \tilde{g}_{\phi NN}^2 = 2.86 \pm 0.01. \tag{16}$$

The effective couplings $\tilde{g}_{\phi NN}^i$ are quite different from the $g_{\phi NN}^i$ for scenarios (a) and (b) in Table 1. Consequently, we conclude that the $K\bar{K}$ -continuum is not well represented by a vector meson dominance approximation. Note, however, that $\tilde{g}_{\phi NN}^2$ is comparable to $g_{\phi NN}^2$ as obtained from the pole analysis [12]. The reason for this “agreement” will be discussed in the next section.

In deriving values for the $g_{\phi NN}^i$ from KN data, we note that there exist un-quantified theoretical uncertainties beyond those quoted in Table 1. A more careful treatment of

the $b_1^{\lambda_1, \lambda_2}$ would have included form factors along with simple coupling constants in Eqs. (12, 13). Ideally, one would want to follow the lines of Ref. [9] where this has been done for the 2π contribution to the nucleon's isovector form factors and the ρNN vertex. However, the latter treatment relies strongly on the fact that the phases of $\pi\pi \rightarrow N\bar{N}$ scattering and the pion electromagnetic form factor essentially follow each other because the inelasticities are small. Unfortunately, the situation is more complicated in the kaon case, and a straightforward extension of the method of Ref. [9] is not possible.

Hence, there is an error bar associated with our ϕNN couplings due to the continuum under the peak which we are unable to quantify at this time. Nevertheless, an important difference between isoscalar and the isovector case is that the width of the resonance peak is much smaller in the former. Consequently, non-resonant continuum effects are not likely to substantially affect the residue for such a pronounced resonance. This expectation is corroborated by the fact that the coupling constants do not change appreciably with the width (scenario (a) vs. (b)).

Finally, we observe that since the amplitudes themselves – rather than a parametrization of them – is used in Eqs. (2, 3, 7, 8), the interpretation of the $b_1^{1/2, \pm 1/2}$ is inconsequential for the following form factor analysis.

4 Form Factor Fits

We now include the $K\bar{K}$ -continuum into the dispersion analysis of the isoscalar electromagnetic nucleon form factors by adding it to Eqs. (5, 6). We then refit the residues of the ω , ϕ , and S' poles. The masses $m_\omega^2 = 0.6115 \text{ GeV}^2$, $m_\phi^2 = 1.0384 \text{ GeV}^2$, and $m_{S'}^2 = 2.56 \text{ GeV}^2$ are fixed [12]. Since Ref. [8] does not give the phase of the $K\bar{K}$ -continuum relative to the pole contributions, we determine this phase from the fits as well. For simplicity, we do not fit to the experimental data but rather to the results of Ref. [12].⁵ The fits indicate a relative phase of $0 (\pi)$ between the $K\bar{K}$ -continuum and the ω pole contribution for $F_1 (F_2)$. In fact, it is impossible to obtain a satisfactory fit with a different relative phase between the two contributions. After having fixed the relative phase, we aim to determine how much of the original ϕ strength can be accounted for by the $K\bar{K}$ -continuum.

We have performed fits for $F_1^{(I=0)}$ and $F_2^{(I=0)}$ in a number of different scenarios. We present the following four in detail:

- (i) ω , ϕ , and S' poles and no $K\bar{K}$ -continuum (cf. Ref. [12]).
- (ii) ω , ϕ , and S' poles and $K\bar{K}$ -continuum.

⁵Note that in Ref. [12] all form factors have been fitted simultaneously. Since we are mainly interested in qualitative features, we deem this procedure here unnecessary.

Scenario	$g_{\omega NN}^1$	$g_{\phi NN}^1$	$a_{S'}^1$	$a_{\omega'}^1$	$g_{\omega NN}^2$	$g_{\phi NN}^2$	$a_{S'}^2$	$a_{\omega'}^2$
(i)	21.1	-9.7	0.0035	-	-3.36	1.98	-0.038	-
(ii)	21.2	-10.7	-0.072	-	-3.31	-0.46	-0.11	-
(iii)	13.1	-	-1.08	-	-3.72	-	-0.142	-
(iv)	19.1	-	0.21	-1.01	-3.42	-	-0.104	-0.04

Table 2: Fitted residues a_V^i for scenarios (i)-(iv). The residues a_V^i are given in units of GeV^2 . For the ω and ϕ poles the couplings $g_{VNN}^i = \frac{f_V}{m_V} a_V^i$ with $f_\phi = 13$ and $f_\omega = 17$ are shown instead of the residue.

(iii) ω and S' poles and $K\bar{K}$ -continuum.

(iv) ω , ω' , and S' poles and $K\bar{K}$ -continuum.

The ω' pole in scenario (iv) is not physical. It was introduced in Ref. [17] to parametrize the contribution of the $\rho\pi$ -continuum obtained from the Bonn potential. We take the same mass, $m_{\omega'} = 1.2544 \text{ GeV}^2$, as in Ref. [17]. However, we let the residue free because our $K\bar{K}$ -continuum is different from the one used in Ref. [17]. The results of the fits are shown in Table 2. Scenario (i) corresponds to the original analysis of Ref. [12]. In the other scenarios the strong ϕ coupling demanded by the data is partially or fully accounted for by the $K\bar{K}$ -continuum or the $\rho\pi$ -continuum (modelled by the effective ω' pole). Most of the fits give a similarly accurate description of the form factors from Ref. [12]. The fit for scenario (iii) is somewhat poorer because there is one fitparameter less.

We now make several observations based on the fits. In particular, the ω contribution is very stable in all scenarios. However, this is not the case for the residual ϕ and the S' . Since the S' is not a physical vector meson but effectively summarizes higher lying strength this is neither surprising nor alarming.

To understand the role of the ϕ , consider in detail $F_2^{(I=0)}$: when the $K\bar{K}$ -continuum is introduced in scenario (ii), the ϕNN coupling is reduced considerably. In fact, in scenarios (iii) and (iv) the form factor can be described without a ϕ pole at all. Consequently, all the ϕ strength can be accounted for by either the $K\bar{K}$ -continuum alone or in tandem with a small, effective $\rho\pi$ -continuum contribution. This is the reason why the effective coupling $\tilde{g}_{\phi NN}^2$ from the previous section is comparable to $g_{\phi NN}^2$ from Ref. [12] (even though the effective coupling $\tilde{g}_{\phi NN}^2$ is not the same as the tensor coupling extracted from the KN partial waves).

The situation is different, however, for $F_1^{(I=0)}$: when the $K\bar{K}$ -continuum is introduced in scenario (ii), the ϕNN coupling is almost unchanged. This suggests additional contributions in the ϕ region that are mocked by the S' in scenario (i). Further evidence is provided by scenario (iii): removing the ϕ pole significantly changes the otherwise very

stable ωNN coupling by a factor of 2 and leads to a unnaturally large coupling for the S' . If the ϕ , however, is replaced by the ω' as in scenario (iv), reasonable couplings for the ω and S' are obtained. In contrast to $F_2^{(I=0)}$ there appears to be a considerable contribution from the $\rho\pi$ -continuum to $F_1^{(I=0)}$, and the ϕ can not be accounted for by the $K\bar{K}$ -continuum alone.

We conclude that the role of the ϕ in $F_2^{(I=0)}$ is well understood, and that it cannot be represented by a simple VMD structure with the physical ϕ nucleon couplings. The role of the ϕ in $F_1^{(I=0)}$ remains ambiguous. This ambiguity stems from the fact that (a) the $K\bar{K}$ contribution does not saturate the spectral function strength in the ϕ -region and (b) equally acceptable fits are obtained whether one saturates this strength either with a ϕ pole explicitly or with an effective $\rho\pi$ (ω') pole. Moreover, the flavor structure of the latter is also open to debate, since the $\rho\pi$ isoscalar EM and strangeness form factors contain ϕ -strength [18, 26]. We suspect, nevertheless, that nearly all of the strength in $t \approx 1 \text{ GeV}^2$ region is due to the ϕ , since the values of $g_{\phi NN}^1$ obtained in scenarios (i) and (ii) agree with the values obtained from the KN partial waves.

5 Strange Moments

Finally, we use the fits from above to obtain information on the leading strange moments,

$$\kappa^s = F_2^s(0), \quad \text{and} \quad \langle r^2 \rangle_D^s = 6 \frac{dF_1^s(t)}{dt} \Big|_{t=0}. \quad (17)$$

In pole models [15, 20, 21], the couplings of the ϕ and ω to the strange vector current are inferred from their known flavor content and coupling to the isoscalar electromagnetic current. The ratios of the corresponding pole residues are [15, 18]

$$(a_\omega^i)^s / a_\omega^i = -\sqrt{6} \left[\frac{\sin \epsilon}{\sin(\epsilon + \theta_0)} \right] \approx -0.2, \quad (18)$$

$$(a_\phi^i)^s / a_\phi^i = -\sqrt{6} \left[\frac{\cos \epsilon}{\cos(\epsilon + \theta_0)} \right] \approx -3, \quad (19)$$

where the superscript s denotes the residue for the strangeness form factor, $\theta_0 = 0.6154$ is the “magic” octet-singlet mixing angle giving rise to pure $u\bar{u} + d\bar{d}$ and $s\bar{s}$ states and $\epsilon = 0.055$ deviations from ideal mixing. Since the flavor content of the S' is not known, its coupling to the strange current was fixed by an asymptotic condition. Here, we follow a slightly different approach.

We consider scenarios (i) and (ii) from Section 4 corresponding to ω , ϕ , and S' poles without and with $K\bar{K}$ -continuum, respectively. The residues of the ω and ϕ poles have been obtained from fits to the isoscalar form factors in the previous section. As in Refs. [15, 20, 21], we draw upon simple flavor rotation arguments leading to Eqs. (18, 19)

to determine the corresponding residues for the strange vector form factors. The $K\bar{K}$ contribution is also known [8] and its phase has been determined from fits to the electromagnetic form factors. For illustrative purposes, we also consider scenario (iv), under the assumption that the intermediate $3\pi \leftrightarrow \rho\pi$ state (parameterized as the ω' in Ref. [17]) does not couple to $\bar{s}\gamma_\mu s$. Although the latter *ansatz* is not well-justified phenomenologically [18, 26], we include it to demonstrate the sensitivity of our predictions to rather extreme assumptions.

The combined contributions from the ω -resonance, $K\bar{K}$ continuum, and residual ϕ -strength to the strangeness moments are listed in Table 3 as the “low-mass” values for the moments. These contributions are strongly constrained by the phenomenology of EM form factor data, KN scattering phase shifts, $e^+e^- \rightarrow K\bar{K}$ cross sections, and vector meson flavor content. It is difficult to maintain consistency with these phenomenological inputs and evade the low-mass contribution to the strangeness moments given in Table 3. One might have expected the use of scenario (iv) – where the ϕ strength is replaced by the effective $\rho\pi$ contribution – to yield smaller low-mass values. In fact, the low-mass value for κ^s under scenario (iv) is similar to the other values in Table 3, since the effective $\rho\pi$ contribution to $F_2^{(I=0)}$ is negligible and since the $K\bar{K}$ contribution saturates the ϕ -strength. In the case of $\langle r^2 \rangle_D^s$, the impact is potentially more significant. If one assumes the resonating $\rho\pi$ do not couple to the strange vector current, the scenario (iv) prediction for $\langle r^2 \rangle_D^s$ has a smaller magnitude and opposite sign to the scenario (i) and (ii) predictions. The assumption that $\langle 0|\bar{s}\gamma_\mu s|\rho\pi\rangle = 0$, however, is inconsistent with the phenomenology of ϕ decay, which displays a 13% branch to $\rho\pi$. To the extent that the $\rho\pi$ vector current form factors are ϕ -meson dominated [26], the $\rho\pi$ contribution to the nucleon isoscalar EM and strangeness moments should obey the relation in Eq. (19). Consequently, a more realistic scenario (iv) low-mass value for $\langle r^2 \rangle_D^s$ should be closer to those from the other scenarios.

The remaining – and dominant – uncertainty is associated with the higher-mass content of the spectral functions. In the VMD approach, the effect of higher mass states is parameterized by a single S' pole. Whether this pole represents a single resonance with an in-principle well-defined flavor wavefunction or a sum over a tower of higher mass states (*viz.*, $KK\pi$, $KK\pi\pi\ldots\Lambda\bar{\Lambda}\ldots$) is uncertain. Consequently, in the earlier works [15, 20, 21] its contribution to the strange spectral function was fixed by requiring specific asymptotic behavior ($t \rightarrow \infty$) for the form factors. The choice of this condition is somewhat ambiguous, however, and the leading strange moments vary strongly for different reasonable choices for this condition [21, 22].

We suggest an alternative method to quantify the uncertainty associated with the unknown higher mass spectral content. First, we argue that a purely hadronic description of the form factors is applicable only for relatively small momentum transfers (*e.g.*, $|t| \leq \text{a few } (\text{GeV}/c)^2$). From the standpoint of quark-hadron duality, we would expect a hadronic approach to produce the asymptotic t -dependence obtained from quark counting

Moment	Scenario	<i>low-mass value</i>	<i>reasonable range</i>
κ^s	(i)	-0.43	$-0.39 \rightarrow -0.48$
	(ii)	-0.28	$-0.15 \rightarrow -0.41$
	(iv)	-0.39	$-0.26 \rightarrow -0.51$
$\langle r^2 \rangle_D^s [\text{fm}^2]$	(i)	0.42	0.42
	(ii)	0.42	$0.41 \rightarrow 0.43$
	(iv)	-0.15	$-0.13 \rightarrow -0.17$

Table 3: *Low-mass value* and *reasonable range* for the leading strange moments κ^s and $\langle r^2 \rangle_D^s$ as defined in the text.

rules only when a sum over the entire hadronic spectrum is carried out. At present, performing this sum is not feasible. Consequently, a hadronic framework should adequately describe the form factor only over a finite range of momentum transfer, as is used in the fits of the isoscalar EM form factors.

Second, we assume that for each higher mass intermediate state, some relation exists between its contribution to the isoscalar EM and strangeness spectral functions. Roughly speaking, the “maximal” relation is given by Eq. (19): whatever a state does in the isoscalar EM channel, it does about three times more strongly in the strangeness channel. States which do not contain resonating $s\bar{s}$ pairs would give relatively weaker contributions to the strangeness spectral function. Using a single S' pole to characterize the higher-mass spectral content, the largest higher-mass effect would be given by assuming the ratio of its residues $(a_{S'}^i)^s/s_{S'}^i$ is given by Eq. (19). We obtain a “reasonable range” for the strangeness moments by adding and subtracting this maximal S' contribution to the low-mass values in Table 3.⁶ Leaving the sign of the S' uncertain allows for the possibility of cancellations between higher-mass contributions to the isoscalar EM spectral function which do not persist in the strangeness channel.

In Table 3 we show our results for scenarios (i), (ii), and (iv) (under the extreme assumptions for the $\langle 0|\bar{s}\gamma_\mu s|\rho\pi\rangle$ discussed above). We observe that both magnitude and sign for κ^s are relatively robust. Differing assumptions for the higher mass contribution lead to at most a factor of 2-3 variation in the magnitude of κ^s but no variation in the phase. It is difficult to generate a positive sign for κ^s under any scenario and maintain consistency with the phenomenological constraints discussed earlier. The predictions for the strange radius are less certain. Although the reasonable ranges for $\langle r^2 \rangle_D^s$ are generally smaller than those for κ^s , the low-mass value depends strongly on one’s assumptions about the $3\pi \leftrightarrow \rho\pi$ coupling to $\bar{s}\gamma_\mu s$. We emphasize, however, that the result for scenario (iv)

⁶Note that the case when the S' is identified with the $\omega(1600)$ and couples according to Eq. (18) is contained in this range.

appearing in Table 3 is likely to underestimate the magnitude of the radius, given the phenomenology of ϕ decays.

Should the experimental value for either of the strangeness moments lie outside our reasonable range by more than one standard deviation, we would conclude that our treatment of the higher mass contributions is too naïve. In this respect, the first results for κ^s from the SAMPLE collaboration [27] are suggestive. It is conceivable, for example, that states such as the $KK\pi$ could give resonance enhanced contributions to the strangeness form factors but only small effects in the isoscalar form factors (see *e.g.*, the initial studies of higher mass contributions in Ref. [28]). Such a scenario might arise from the presence of two opposite sign pole contributions to the $KK\pi$ EM form factor (*e.g.*, $\omega(1600)$ and $\phi(1680)$) which do not both appear in the $KK\pi$ strangeness form factor (*e.g.*, $\phi(1680)$ only). At present, such scenarios remain speculative and await a more detailed analysis of the higher mass strangeness spectral content.

6 Conclusions

The spectral content of the isoscalar EM form factors appears to be considerably more complex than that of the isovector form factor. Only recently, for example, has the connection between continuum and resonant contributions to $F_1^{(I=0)}$ and $F_2^{(I=0)}$ been elucidated [29, 8]. In order to address some of the open questions regarding the isoscalar spectral content, we have drawn upon our previous study of the $K\bar{K}$ continuum [29, 8] in the present reanalysis of the isoscalar form factors. The relative phase between the $K\bar{K}$ contribution and the vector meson poles has been determined from the electromagnetic fits. We have then refitted the residues of the ω , ϕ , and higher mass (S') poles in various scenarios in order to determine how much of the ϕ strength demanded by the data can be accounted for by the $K\bar{K}$ -continuum. Our main findings are as follows:

- (a) the relative phase between $K\bar{K}$ -continuum and ω pole contribution is $0(\pi)$ for $F_1(F_2)$,
- (b) the ω contributions to the form factors are stable with respect to differing treatments of other contributions,
- (c) for $F_2^{(I=0)}$ all of the ϕ strength is accounted for by the $K\bar{K}$ -continuum while for $F_1^{(I=0)}$ additional ϕ strength (*e.g.* via $3\pi \rightarrow \rho\pi \rightarrow \phi$) is needed,
- (d) the $K\bar{K}$ contribution to the form factors is ϕ -resonance enhanced yet is not well represented by a vector meson dominance approximation.

Furthermore, we have determined the ϕNN coupling constants from the form factor fits and directly from the $K\bar{K} \rightarrow N\bar{N}$ partial waves. The extracted coupling constants (cf. Tables 1, 2) imply large OZI-violation. As observed previously for the ωNN couplings [2], the results of the two methods do not agree. For a variety of reasons discussed above, we deem it more sensible to extract the couplings directly from the partial waves.

We have also developed the implications for the leading moments of the nucleon's strange vector form factors. We quantify the main uncertainty in this approach by splitting the leading moments into low-mass and higher mass contributions. We quote a *low-mass value* that consists of the reasonably well known ω , ϕ , and $K\bar{K}$ contributions. These contributions are strongly constrained by isoscalar EM form factor data, KN partial waves, $e^+e^- \rightarrow K\bar{K}$ cross sections, and vector meson octet phenomenology. We also give a *reasonable range* by considering the scenarios in which the remaining higher-mass intermediate state contributions, parameterized by a single vector meson pole S' , couples to strangeness maximally like the ϕ (or with an opposite sign). We find that both the magnitude and negative sign for κ^s are rather robust for various scenarios, whereas the predictions for $\langle r^2 \rangle_D^s$ contain more variation. Whether there exist additional higher-mass contributions which would modify our reasonable ranges for the strangeness moments yet which do not affect the isoscalar EM form factors remains to be seen.

Acknowledgement

We wish to thank T. Cohen, R.L. Jaffe, and U.-G. Meißner for useful discussions. HWH acknowledges the hospitality of the Institute for Nuclear Theory in Seattle where part of this work was carried out. MJR-M has been supported in part under U.S. Department of Energy contract # DE-FG06-90ER40561 and under a National Science Foundation Young Investigator Award. HWH has been supported by the Natural Sciences and Engineering Research Council of Canada.

References

- [1] M. Weitz et al., Phys. Rev. Lett. 72 (1994) 328; D.J. Berkeland et al., Phys. Rev. Lett. 75 (1995) 2470.
- [2] D. Drechsel et al., Hadron Polarizabilities and Form Factors: Working Group Summary, in: Chiral Dynamics: Theory and Experiment, A.M. Bernstein, D. Drechsel, and T. Walcher (eds.), Lecture notes in physics (Vol. 513), Springer, 1998, [nucl-th/9712013].
- [3] G. Quémener et al., presented at INPC 98, Aug. 24-28, 1998, Paris, France.

- [4] P. Federbush, M.L. Goldberger, and S.B. Treiman, Phys. Rev. 112 (1958) 642.
- [5] G.F Chew et al. , Phys. Rev. 110 (1958) 265.
- [6] S.D. Drell and F. Zachariasen, Electromagnetic Structure of Nucleons, Oxford University Press, 1961.
- [7] M.J. Musolf, H.-W. Hammer, and D. Drechsel, Phys. Rev. D55 (1997) 2741.
- [8] H.-W. Hammer and M.J. Ramsey-Musolf, preprint TRI-PP-98-26, [hep-ph/9812261].
- [9] G. Höhler and E. Pietarinen, Nucl. Phys. B95 (1975) 210.
- [10] J.J. Sakurai, Currents and Mesons, University of Chicago Press, Chicago, 1969.
- [11] G. Höhler et al., Nucl. Phys. B114 (1976) 505.
- [12] P. Mergell, U.-G. Meißner, and D. Drechsel, Nucl. Phys. A596 (1996) 367; H.-W. Hammer, U.-G. Meißner, and D. Drechsel, Phys. Lett. B385 (1996) 343.
- [13] W.R. Frazer and J.R. Fulco, Phys. Rev. 117 (1960) 1603, *ibid.* 1609.
- [14] S. Okubo, Phys. Lett. 5 (1963) 165; G. Zweig, CERN Report No. 8419 TH 412 (1964); J. Iizuka et al., Prog. Theor. Phys. 35 (1966) 1061.
- [15] R.L. Jaffe, Phys. Lett. B229 (1989) 275.
- [16] V. Bernard, N. Kaiser, and U.-G. Meißner, Nucl. Phys. A611 (1996) 429.
- [17] U.-G. Meißner, V. Mull, J. Speth, and J.W. van Orden, Phys. Lett. B408 (1997) 381.
- [18] H.-W. Hammer and M.J. Ramsey-Musolf, Phys. Lett. B416 (1998) 5.
- [19] Particle Data Group, Review of Particle Properties, Eur. Phys. J. C 3 (1998) 1.
- [20] H.-W. Hammer, U.-G. Meißner, and D. Drechsel, Phys. Lett. B367 (1996) 323.
- [21] H. Forkel, Prog. Part. Nucl. Phys. 36 (1996) 229; H. Forkel, Phys. Rev. C56 (1997) 510.
- [22] M.J. Musolf, talk given at the European Research Conference on “Polarization in Electron Scattering”, Santorini, Greece, September 12 - 17, 1995; M.J. Musolf, lectures given at the “11th Student’s Workshop on Electromagnetic Interactions”, Bosen, Germany, September 1994.
- [23] R.A.W. Bradford and B.R. Martin, Z. Phys. C 1 (1979) 357.

- [24] F. Felicetti and Y. Srivastava, Phys. Lett. B107 (1981) 227.
- [25] I. Sabba-Stefanescu, J. Math. Phys. 21 (1980) 175.
- [26] J.L. Goity and M.J. Musolf, Phys. Rev. C53 (1996) 399.
- [27] B. Mueller et al., SAMPLE Collaboration, Phys. Rev. Lett. 78 (1997) 3824.
- [28] L.L. Barz, H. Forkel, H.-W. Hammer, F.S. Navarra, M. Nielsen, M.J. Ramsey-Musolf, Nucl. Phys. A640 (1998) 259.
- [29] M.J. Ramsey-Musolf and H.-W. Hammer, Phys. Rev. Lett. 80 (1998) 2539.